

# Automated lower bound analysis of concrete slabs

C. J. Burgoyne\* and A. L. Smith†

University of Cambridge; Steel Construction Institute

*A method is developed that allows automated lower bound analyses of concrete slabs to be carried out, with the specific aim of producing a technique that can be applied to existing structures which are being assessed after many years in use and for which the original calculations, and hence the assumed methods of load distribution, have been lost. It is shown that any load distribution within the slab can be expressed in terms of an equilibrium state and a set of states of self-stress. Optimisation techniques are developed that allow the highest lower bound to be found. It is shown that an analysis based on the original Hillerborg two-strip model fails to find a reasonable lower bound when the slab is subjected to point loads and in the corners of slabs but a refinement using four sets of strips at 45° to each other can give very good agreement with both exact analytical solutions and upper bound methods.*

## Notation

<b>A</b>	equilibrium equations matrix	$R_L, R_R$	reactions at left- and right-hand ends of strip
$a, b, u, v$	directions of four-strip systems (Fig. 19)	<b>S</b>	matrix of states of self-stress
<b>a–j</b>	letters defining individual strips	$w_i$	distributed load acting on length $L_i$ of strip
<b>b</b>	column vector of load terms from equilibrium equations	$x, y$	directions
<b>e</b>	column vector of equilibrium state	$a$	proportion of $q$ carried in x-direction strips
$L$	length of side of slab	$\lambda$	vector of magnitudes of states of self-stress
$L_i$	length of distributed load on a strip (Fig. 3)		
$M_a, M_b, M_u, M_v$	moments in strips defined by $a, b, u, v$		
$M_L, M_R$	moments at left- and right-hand ends of strip		
$m_p$	flexural moment capacity		
$M_x, M_y, M_{xy}$	applied moments (defined in Fig. 1)		
$p, p_i$	self-equilibrating inter-strip force		
<b>p*</b>	column vector of self-equilibrating forces		
$q$	distributed load		
$Q, Q_{max}$	total distributed load		
$q_i$	distributed load (dimensionless)		

## Introduction

The problems caused by using different methods for the design of concrete slabs, and their subsequent re-analysis for assessment, have been highlighted in an earlier paper.<sup>1</sup> If the original calculations have been lost, it is common for structures to be condemned because the checker does not know the original designer's logic.

In many cases the design would have been carried out by hand calculation, often using the Hillerborg strip method<sup>2,3</sup> or code rules that were derived from it. That method assumes a distribution of load between two sets of strips, usually orthogonal, for which the reinforcement can then be designed independently. The engineer's choice of load distribution is arbitrary, and the resulting moments may differ from those in the real structure, but the lower bound theorem of plasticity<sup>4</sup> means that the structure will be safe. As long as the engineer has provided sufficient reinforcement for the

\* Department of Engineering, University of Cambridge, Trumpington Street, Cambridge, CB2 1PZ, UK

† Steel Construction Institute, Silwood Park, Ascot, Berkshire, SL5 7QN, UK

(MACR-D-07-00005) Paper received 20 December 2006; last revised 21 February 2008; accepted 13 March 2008

moments that have been calculated, and has complied with normal code rules to ensure ductility, the difference between the actual and assumed moments does not matter. The worst that could happen is that the structure would crack prematurely in the under-strength direction, but it would be strong enough in the other direction and the structure would be safe.

The problem is that the checker does not know how the original designer chose to distribute the loads, or even what type of analysis was performed. Modern finite element packages are now so easy to use, at least in their linear elastic incarnations, and give such pretty pictures as output, that the analyst is tempted to believe that the results are precise. Many structures are being wrongly condemned. May and Mann (personal communication) have recently shown that a fully non-linear finite element analysis does allow the post-cracking and post-yield behaviour of the slab to be followed, but the use of such programs requires expert knowledge and is not undertaken in routine assessment.

There have been attempts to automate the use of the plasticity bound theorems for design and analysis. Middleton<sup>5</sup> has developed a technique to automate the yield line method, primarily aimed at the assessment of bridge decks. He uses a library of possible failure mechanisms whose parameters are altered to obtain the lowest upper bound. He has conducted many tests to show that, despite being an upper bound, his predictions are sufficiently close to the true collapse load that they can be used as the basis for an assessment of structural safety. It has also been observed that membrane forces are frequently developed which cause the final collapse load to be above the upper bound prediction. Nevertheless fears are still expressed that the results are on the unsafe side, by definition.

The Hillerborg strip method has been automated before by O'Dwyer and O'Brien,<sup>6</sup> using a technique that differs from the one presented here. Both techniques are satisfactory as design tools, but the Hillerborg approach itself has to be modified for use as an analysis tool.

What is needed is a method that can be used to automate the lower bound method for use in analysis, so that the highest lower bound can be compared with the lowest upper bound. Even though neither method gives the true collapse load, if the two bounds differ by only a small amount the checker could have confidence in the judgement that is made of the slab's capacity. The current paper presents a method to address that problem.

### Sign convention

Figure 1 shows the sign convention used for moments, which is consistent with that used for most reinforced concrete slab work. As defined, positive moments relate to hogging moments and are thus resisted by the top steel in a slab and  $M_x$  refers to moments resisted by steel running in the  $x$ -direction and not to

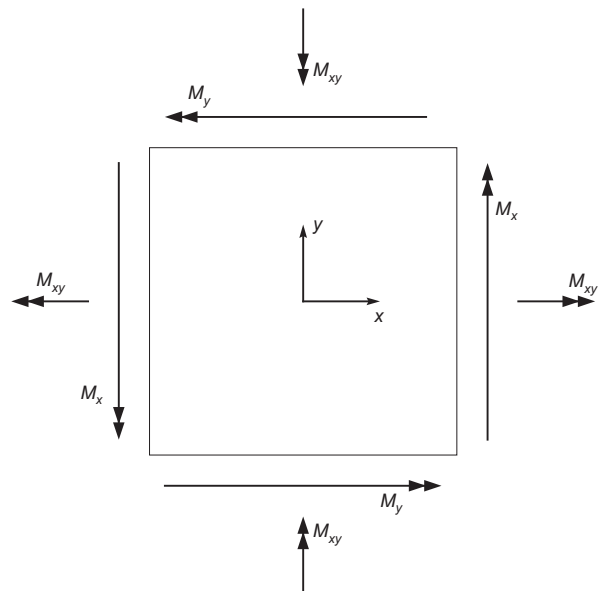


Fig. 1. Sign convention for moments

moments about the  $x$ -axis. In most cases, rigour of sign convention is not required, and reference will be made to sagging and hogging moments, and to longitudinal strips (which run in the  $x$ -direction) and transverse strips (which run in the  $y$ -direction). The method can easily be adapted to any other self-consistent sign convention.

### Hillerborg strip method

The standard Hillerborg strip method assumes that the slab is made up of two sets of intersecting strips; they will be taken here to be orthogonal but the extension to non-orthogonal strips is straightforward. The basic equilibrium equation for flexure of a plate is

$$\frac{\partial^2 M_x}{\partial x^2} - 2 \frac{\partial^2 M_{xy}}{\partial x \partial y} + \frac{\partial^2 M_y}{\partial y^2} = q \quad (1)$$

Hillerborg chose to make  $M_{xy}$  zero, which allowed a simpler equilibrium system to be set up in which the applied load  $q$  could be shared between the two strips with  $\alpha q$  applied to one strip and  $(1-\alpha)q$  applied to the other strip. He was almost certainly aware that resisting  $M_{xy}$  moments is also more costly in reinforcement. The equilibrium equations for the two strips could then be separated.

$$\begin{aligned} \frac{\partial^2 M_x}{\partial x^2} &= \alpha q \\ \frac{\partial^2 M_y}{\partial y^2} &= (1 - \alpha)q \end{aligned} \quad (2)$$

The reinforcement in each strip can be designed on the basis of beam theory: if the strips are designed in accordance with normal code rules the strips will be

under-reinforced and will fail in flexure before they fail in shear. The lower bound theorem of plasticity applies and the structure will be safe whatever value of  $\alpha$  has been chosen. In practice, codes often specify how the load is to be distributed, using ‘column strips’ and ‘middle strips’, but these requirements are designed to prevent early cracking of the slab and are not required for safety.

As originally proposed, the method cannot deal with patch loads, since many strips will be unloaded, but a set of self-equilibrating forces  $p$  can be introduced between the two sets of strips whose total external effect is zero. This would leave the designer with two parameters  $\alpha$  and  $p$  that can be chosen at will, but without any loss of generality, the problem can be simplified by setting  $\alpha$  to unity (thus applying all the load to the strips in the  $x$ -direction) and using  $p$  to specify how the load is transferred within the slab.

$$\begin{aligned} \frac{\partial^2 M_x}{\partial x^2} &= q + p \\ \frac{\partial^2 M_y}{\partial y^2} &= -p \end{aligned} \quad (3)$$

As described above, the method is suitable for design. The problem now is to reverse the usual process so that an existing structure can be analysed. Instead of choosing  $p$ , and then calculating the required moment capacities  $m_x$  and  $m_y$ , a method is needed to find the  $p$  values for a slab with a known moment capacity. This is much more complex; the design problem leads directly to a solution, whereas the inverse problem requires searching for optimal values of  $p$ , and there are many more of these than there are pattern parameters in the normal yield line analysis.

### The method

Consider a rectangular slab divided into orthogonal regions, as shown in Fig. 2, which defines two sets of strips. The applied load and moment capacities are assumed to be constant within each region, and the boundary conditions for the strips are constant for each set of strips. The moments in the strips can be completely defined by the values of  $p_i$  assigned to each rectangular region.

The objective is to determine a distributed load,  $Q_{max}$  (dimensions  $FL^{-2}$ ) that can be multiplied by the dimensionless load distribution,  $q_i$ , which describes how the load is applied to the slab, to give the predicted maximum loading for the structure,  $Q_{max}q_i$ . The loads applied to the longitudinal strips are thus  $Q_{max}(q_i + p_i)$  and those on the transverse strips  $-Q_{max}p_i$ . The values of  $q_i$  are known but the  $p_i$  have to be determined subject to the condition that the moment capacity in each strip, in either hogging or sagging bending, cannot be exceeded.

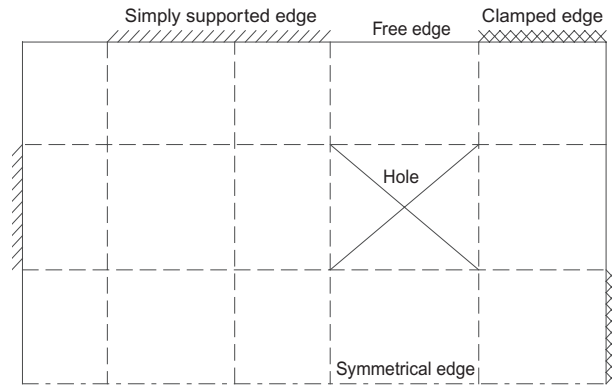


Fig. 2. Typical general slab showing notation for boundary conditions. Moment capacities and loads are constant within each rectangular region

Allowance has to be made for the support conditions for a strip. A general strip (Fig. 3) has up to four end reactions or moments; depending on the type of support some of these may be zero or there will be additional equilibrium equations that have to be satisfied.

For a strip that is fixed at both ends,  $M_L$  and  $M_R$  can take any values and it will still be possible to determine  $R_L$  and  $R_R$  using the two equations of overall equilibrium for the strip. However, if the right-hand end is free, the left-hand edge moment,  $M_L$ , will have a fixed relationship to the applied loads,  $w_i$ , in order for overall equilibrium to be satisfied.

For a strip that is free at both ends the applied loads themselves will have to satisfy both vertical and moment equilibrium so that all the end reactions and moments are zero. In both cases the edge moment for a free end will be set to zero.

By considering every strip that makes up the complete slab and replacing  $w_i$  with the loads given by equation (3) a set of simultaneous equations can be derived that defines an equilibrium system for the slab. This can be expressed in matrix form as

$$A p^* = b \quad (4)$$

$p^*$  is a column vector of internal loads,  $p_i$ , and the non-zero edge moments;  $A$  and  $b$  are the matrix and column vector that contain the terms from the simultaneous equations described above.  $A$  holds the values that relate to the entries in the  $p^*$  vector and  $b$  holds the values that relate to the applied loads,  $q_i$ . Equation (4) defines the equilibrium of the system, and by using values for  $p^*$  that satisfy this equation the support conditions will always be satisfied.

The shape of the matrix  $A$  depends on the degree of statical indeterminacy. If the system is determinate the

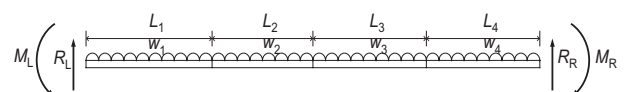


Fig. 3. Notation for loading on strip

matrix will be square and the moment distribution is fixed. Normally **A** will have more columns than rows, reflecting statical indeterminacy, and the solution will take the form

$$\mathbf{p}^* = \mathbf{e} + \mathbf{S}\boldsymbol{\lambda} \quad (5)$$

Here **e** is an equilibrium state of the system while **S** is a matrix composed of a series of column vectors, each of which is a state of self-stress:  $\boldsymbol{\lambda}$  is a column vector of variables which add differing amounts of the states of self-stress to the equilibrium state. Thus the objective is to choose the values of  $\boldsymbol{\lambda}$  that maximise  $Q_{\max}$ . This reduces the number of variables that have to be optimised later, significantly speeding up the process. The method can be extended to deal with columns, holes and lines of symmetry, but details are not given here.

The method can most easily be demonstrated by means of an example. The slab shown in Fig. 4 is divided into eight regions, each of which can be loaded independently by choosing values of  $q_i$ . There are simple supports at edges **a**, **b**, **i**, and **m**, and clamped supports at edges **j** and **k**. In addition to the eight internal forces ( $p_1$  to  $p_8$ ) there will be two edge moments ( $M_j$  and  $M_k$ ), so the vector  $\mathbf{p}^*$  has ten components. Once these are determined, the support reactions and moments in all strips can be calculated. The example is slightly artificial but it shows all aspects of the way the method has been implemented.

To find  $\mathbf{p}^*$ , the matrices **A** and **b** have to be found. The relationship between the variables needs to be determined so that the edge conditions are satisfied. Consider first the longitudinal strip **m**–**e**. To establish equilibrium for this strip the moment applied by the four loads,  $q_i + p_i$ , about edge **m** must be zero, giving

$$(q_1 + p_1) \frac{L^2}{2} + (q_2 + p_2) \frac{3L^2}{2} + (q_3 + p_3) \frac{5L^2}{2} + (q_4 + p_4) \frac{7L^2}{2} = 0 \quad (6)$$

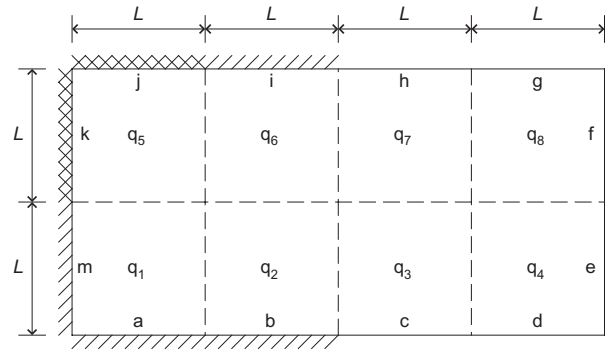


Fig. 4. Example used to demonstrate method. Hatched edges represent simple support; cross-hatched edges represent clamped supports; plain edges represent free edges

Moment equilibrium of strip **k**–**f** gives a similar equation

$$(q_5 + p_5) \frac{L^2}{2} + (q_6 + p_6) \frac{3L^2}{2} + (q_7 + p_7) \frac{5L^2}{2} + (q_8 + p_8) \frac{7L^2}{2} = M_k \quad (7)$$

Transverse strips **a**–**j** and **b**–**i** will be in equilibrium for any value of the applied loads and edge moments as the reaction forces at both ends of both strips can be adjusted, so these need not be taken into account at this stage. For strips **c**–**h** and **d**–**g** the applied loads,  $-p_i$ , will need to satisfy both force and moment equilibrium.

$$-p_3L + -p_7L = 0 \quad (8)$$

$$\frac{-p_3L^2}{2} + \frac{-3p_7L^2}{2} = 0 \quad (9)$$

$$-p_4L + -p_8L = 0 \quad (10)$$

$$\frac{-p_4L^2}{2} + \frac{-3p_8L^2}{2} = 0 \quad (11)$$

There are thus six equations defining ten variables

$$\begin{bmatrix} \frac{L^2}{2} & \frac{3L^2}{2} & \frac{5L^2}{2} & \frac{7L^2}{2} & 0 & 0 & 0 & 0 & 0 & 0 \\ 0 & 0 & 0 & 0 & \frac{L^2}{2} & \frac{3L^2}{2} & \frac{5L^2}{2} & \frac{7L^2}{2} & 0 & -1 \\ 0 & 0 & -L & 0 & 0 & 0 & -L & 0 & 0 & 0 \\ 0 & 0 & \frac{-L^2}{2} & 0 & 0 & 0 & \frac{-3L^2}{2} & 0 & 0 & 0 \\ 0 & 0 & 0 & -L & 0 & 0 & 0 & -L & 0 & 0 \\ 0 & 0 & 0 & \frac{-L^2}{2} & 0 & 0 & 0 & \frac{-3L^2}{2} & 0 & 0 \end{bmatrix} \times \begin{bmatrix} p_1 \\ p_2 \\ p_3 \\ p_4 \\ p_5 \\ p_6 \\ p_7 \\ p_8 \\ M_j \\ M_k \end{bmatrix} = \begin{bmatrix} \frac{-(q_1 + 3q_2 + 5q_3 + 7q_4)L^2}{2} \\ \frac{-(q_5 + 3q_6 + 5q_7 + 7q_8)L^2}{2} \\ 0 \\ 0 \\ 0 \\ 0 \end{bmatrix} \quad (12)$$

All the loading terms are on the right-hand side of this equation, which can be rearranged by Gaussian elimination; pivoting reorders the variables. For a uniform load over the entire slab,  $q_1 = q_2 = \dots = q_8 = q$ , and with  $L = 1$  m, equation (12) becomes

$$\begin{bmatrix} 1 & 0.068 & 0.593 & 0.356 & 0 & 0 & 0.119 & 0 & 0 & -0.237 \\ 0 & 1 & -0.047 & -0.028 & 0.690 & 0.414 & -0.009 & 0.138 & 0 & 0.019 \\ 0 & 0 & 1 & 0.175 & 0.399 & 0.070 & 0.058 & 0.023 & 0 & -0.117 \\ 0 & 0 & 0 & 1 & -0.005 & 0.397 & 0.333 & 0.132 & 0 & -0.667 \\ 0 & 0 & 0 & 0 & 1 & 0.202 & 0 & 0.067 & 0 & 0 \\ 0 & 0 & 0 & 0 & 0 & 1 & 0 & 0.333 & 0 & 0 \end{bmatrix} \begin{bmatrix} p_8 \\ p_4 \\ p_7 \\ p_6 \\ p_3 \\ p_2 \\ p_5 \\ p_1 \\ M_j \\ M_k \end{bmatrix} = \begin{bmatrix} -1.898q \\ -2.058q \\ -1.306q \\ -7.449q \\ -1.075q \\ -5.333q \\ 0 \\ 0 \\ 0 \\ 0 \end{bmatrix} \quad (13)$$

Equation (13) can be partitioned into a square matrix relating to the first six unknowns ( $p_8 \dots p_2$ ), and other terms relating to the remaining unknowns ( $p_5 \dots M_k$ ). The solution of the square matrix gives an equilibrium state, and the remaining four variables are introduced via the states of self-stress. Here, there are six equations in ten variables so the solution will involve four unknown values  $\lambda_i$ , each of which is a multiplier for one state of self-stress. After reordering the variables back to the natural order, the result is

$$\begin{bmatrix} p_1 \\ p_2 \\ p_3 \\ p_4 \\ p_5 \\ p_6 \\ p_7 \\ p_8 \\ M_j \\ M_k \end{bmatrix} = \begin{bmatrix} 0 \\ -5.333q \\ 0 \\ 0 \\ 0 \\ -5.333q \\ 0 \\ 0 \\ 0 \\ 0 \end{bmatrix} + \begin{bmatrix} 0 & 1 & 0 & 0 \\ 0 & -0.333 & 0 & 0 \\ 0 & 0 & 0 & 0 \\ 0 & 0 & 0 & 0 \\ 1 & 0 & 0 & 0 \\ -0.333 & 0 & 0 & 0.667 \\ 0 & 0 & 0 & 0 \\ 0 & 0 & 0 & 0 \\ 0 & 0 & 1 & 0 \\ 0 & 0 & 0 & 1 \end{bmatrix} \begin{bmatrix} \lambda_1 \\ \lambda_2 \\ \lambda_3 \\ \lambda_4 \end{bmatrix}$$

or

$$p^* = e + S\lambda \quad (14)$$

It is worth considering the physical meaning of this equation.

- (a) There is no load on the transverse strips c-h and d-g, as a free-free beam with two regions cannot satisfy both moment and force equilibrium unless both regions carry no load;  $p_3, p_4, p_7$  and  $p_8$  must always be zero. If this had been recognised before the equations were set up, four variables could have been eliminated, as would four equations. The result would still have needed four states of self-stress.
- (b) The internal forces on regions 2 and 6 are used to balance the forces applied on the remaining regions for the longitudinal strips: in other words the entire load is applied to the longitudinal strips, and these are balanced by forces from the transverse strip b-i. Strip a-j carries no load in the initial equilibrium position as defined by the  $e$  vector.
- (c)  $\lambda_1$  and  $\lambda_2$  are multipliers for the first two states of self-stress, as defined by the first two columns of  $S$ . Each refers to a state of self-stress in one of the longitudinal strips which allows the load to be shifted between strip a-j and strip b-i.
- (d) The third column of  $S$  shows that the edge moment  $M_j$  is entirely independent of the applied loads and can take any value, defined by  $\lambda_3$ , without nullifying the equilibrium of the system.
- (e) The fourth state of self-stress, as defined by the final column of the  $S$  matrix, shows that any change to the edge moment  $M_k$  is balanced by a change in the internal load  $p_6$ . An increase in  $M_k$  corresponds to a decrease in the load on strip b-i.

In more complex cases the physical interpretation of the states of self-stress is less obvious, and if the equations had been reordered differently, other variables might have been involved in the equilibrium state.

### Optimisation

The problem has now been reduced to its simplest form. Any combination of the various states of self-stress, as defined by the values of  $\lambda_i$ , will satisfy equilibrium (and all possible equilibrium states can be expressed by equation (14)). The moments anywhere in the strips can be calculated in the normal way and compared with the moment capacity in each strip. The multiplier  $Q$  that can be applied to all the loads  $q_i$  without exceeding the moment capacity for any combination of  $\lambda_i$  can thus be found. By definition, that value of  $Q$  will be a lower bound on the collapse load of the slab, provided that the slab is sufficiently under-reinforced and thus ductile.

To be useful, the highest lower bound has to be found. Many optimisation techniques have been devised and there is a widespread literature; Press *et al.*<sup>7</sup> give a good discussion of the techniques and pitfalls that can arise.

The Simplex algorithm (or a more sophisticated version thereof) is frequently used in cases where the limiting conditions can be expressed as simple functions, because it can lead directly to the optimal solution, but it is not suitable here because yield could occur at any point along a strip. It is thus very difficult to find simple expressions for bounds on the values of  $\lambda_i$ .

An alternative is Powell's method, which is sometimes referred to as the Hill Climbing method. The technique conducts a series of one-dimensional optimisations along various vectors; the states of self-stress are a convenient set of vectors that have already been defined. By starting from the equilibrium state (defined by the vector  $e$ ) a search is made along one of the directions to find the value of  $\lambda_i$  that gives the largest failure load. The process is repeated by moving along another search vector. If the function is smooth the procedure will zigzag its way to a (possibly local) maximum of the function and is reasonably efficient and simple to program.

When attempts were made to apply the technique to simple slab problems, the solution reached different finishing points depending on how the problem was set up. An example is given in Fig. 5, which shows a simply supported slab divided into two longitudinal strips and four transverse strips under a uniformly distributed load. By enforcing the two lines of symmetry the problem can be reduced to two variables, which allows the value of  $Q$  to be visualised for all combinations of  $p_i$ .

The maximum distributed load that the slab can carry for any value of  $p_1$  and  $p_2$  is plotted in Fig. 6. The circles correspond to results where the numerical procedure stopped before reaching the highest point. The surface consists of a series of smooth regions, separated by discontinuities in slope. The finishing points of the optimisation, from different starting

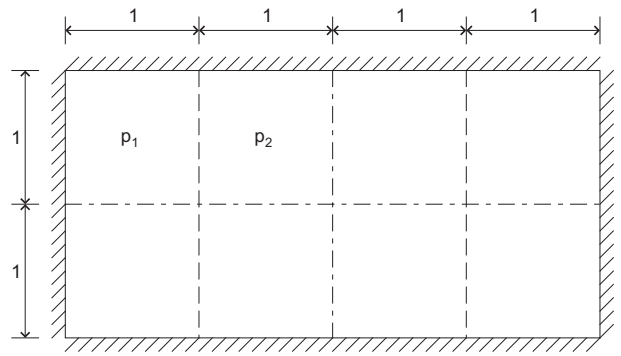


Fig. 5. Two degree-of-freedom problem

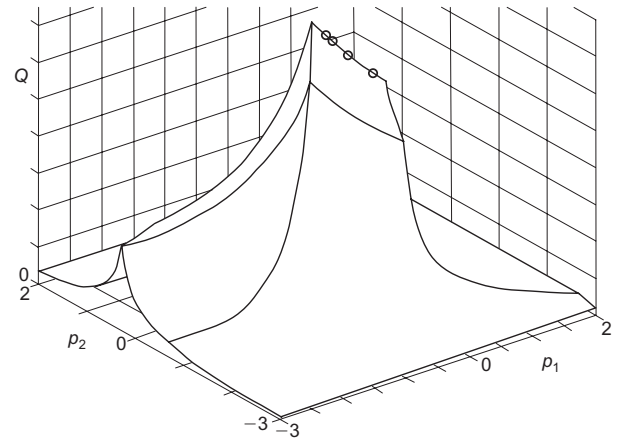


Fig. 6. Slab capacity against  $p_1$  and  $p_2$

points, all lie on one or other of the ridge lines. As an analogy, imagine a climber going up a mountain in fog who is constrained to walk only in N-S or E-W directions. If a point is reached where any step takes the climber downhill, it will be concluded that the summit has been reached. If, however, the climber is on a ridge, running from NE-SW, it may be possible to go higher, but the climber does not realise this.

Figure 7 shows the same surface as a contour plot. Each of the smooth regions corresponds to yield being reached in some, but not all, of the strips. Slope discontinuities occur where these surfaces intersect, and

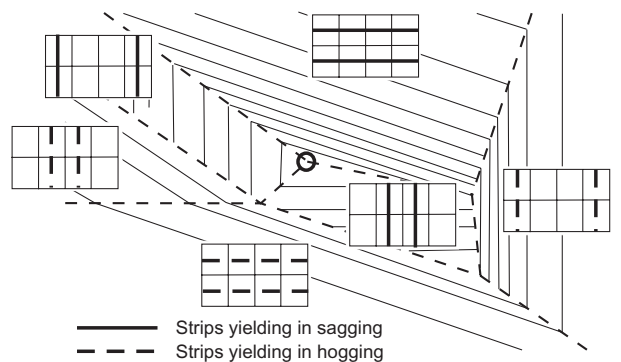


Fig. 7. Contour plot of the two-dimensional surface showing yielded strips (some contours have been omitted for clarity)

some of these discontinuities form ridges. The highest point is reached when several of the ridge lines meet, so to reach the summit the climber has to proceed along the ridge lines. If the iteration technique does not allow movement in these directions, the analysis will stop prematurely. Note that this is not the normal problem associated with reaching a local maximum; stopping on a ridge can occur even if the function has only a single global maximum.

To counteract this effect a modification has been made to the procedure. When the optimisation routine has reached its best estimate of the solution, a jump away is made by randomly choosing a small  $\lambda$  vector to obtain a revised starting point. The optimisation is repeated and it is likely that the new optimum will also be on the same ridge. The line joining the two estimates of the optimum will be on, or near, the ridge line and can be added to the list of search vectors. In the mountaineering analogy the climber would be allowed to walk along the ridge.

In more realistic problems, there will be more variables, so it is less easy to visualise the process, but the optimum solution will still be the one where the largest possible number of strips are yielding, even if it is not always possible for all the strips to yield, and it is still possible to become stuck on a ridge line.

The whole procedure has been automated in a computer program in C++. The software is capable of analysing rectangular slabs, subdivided into rectangular regions with moment capacities specified in the same directions as the strips, and can take account of free, fixed and simply supported edges, and slabs that contain holes, column supports and lines of symmetry. The results presented here are all carried out on the assumption of uniform moment capacity throughout the slab, but it is a trivial extension to vary the moment capacity in different regions to allow for material deterioration or omitted reinforcement, if that were an issue. Extensions to other shapes, and more complex reinforcement

arrangements, would be straightforward but have not been implemented.

### Examples

#### Example 1. Slab designed by strip theory

Figure 8 shows a simply supported slab, of aspect ratio 1.5. A modern assessor might be faced with this type of slab to analyse, but without prior knowledge of the technique used by the original designer. Reynolds and Steedman<sup>8</sup> give a strip design procedure for such a slab, subject to a uniformly distributed load, which leads to the required moment capacities in sagging bending as shown in Fig. 8(a). To demonstrate the power of the method, these moment capacities were used as the starting point, and after a few iterations, the program determined that the load had been distributed as shown in Fig. 8(b). This is precisely the distribution suggested by Reynolds and Steedman.

This example shows that the technique is capable of recovering the assumptions that were made by the original designer. It is the inability to do that with a finite element program that leads to structures being repaired unnecessarily, since the checker is unable to find the load distribution that the original designer found to be adequate. If the original design was adequate before, this method should show that the structure remains adequate. It cannot, however, 'turn a sow's ear into a silk purse'; if the original design was inadequate, or the design load has changed significantly, or the structure has deteriorated with time, it may still fail. The method would still, however, be capable of determining the maximum available capacity.

The method has been checked against other design cases, with similar results. In practice, the reinforcement detailer would usually have made conservative assumptions of capacity, so in many cases it is found

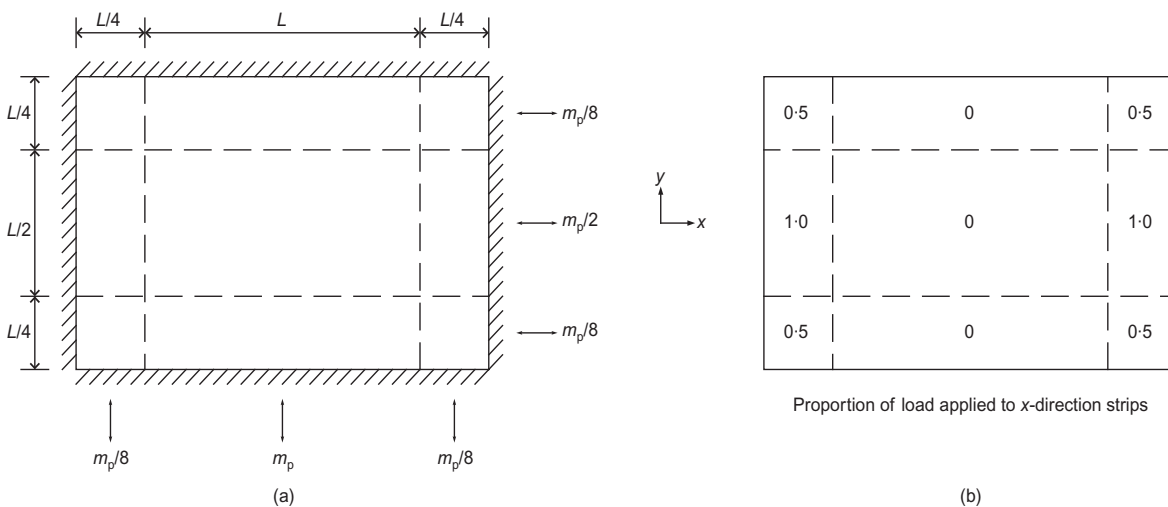


Fig. 8. Layout of slab used in example 1: (a) shows the input moment capacities; (b) shows the load proportions determined by the analysis

that the structure can carry more load than the original designer intended.

It would be possible to stop at this point and be satisfied with a tool that can verify existing good design, and indeed a result such as this could have been achieved, albeit by a different route, using the techniques of O'Dwyer and O'Brien.<sup>6</sup> There are, however, other problems that need to be tackled when assessing existing structures, which show that the method, as explained so far, has limitations.

*Example 2. Short single span with concentrated load*

The second example is of point loads applied to a simply supported, single-span bridge deck. Many such structures are currently being reassessed owing to the requirements for heavier truck loads. The predicted failure patterns for such structures involve partial width yield line patterns with fans. Several physical models of such slabs were tested by Collins.<sup>9</sup> Two of the slabs had limited amounts of reinforcement, but one slab, No. 3, had top and bottom steel in both directions.

The slab layout is shown in Fig. 9; two point loads were applied symmetrically on 30 mm square pads as shown. The maximum load carried by the slab was 31.3 kN (shared between the two loading points), and the final crack pattern on the underside is shown in Fig. 10. Collins carried out yield line analyses of the slab and obtained the lowest upper bound of 25.6 kN for the mechanism shown in Fig. 11, which is clearly a good match to her observed failure mode. She attributed the fact that the slab carried more than its upper bound capacity to strain-hardening in the steel and the development of membrane actions which are known to be important for point loads applied to slabs where compressive arching action can be resisted by ring

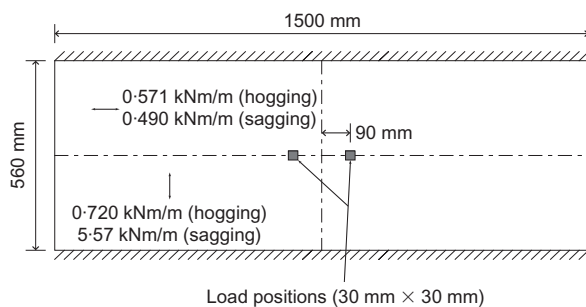


Fig. 9. Collins' slab 3

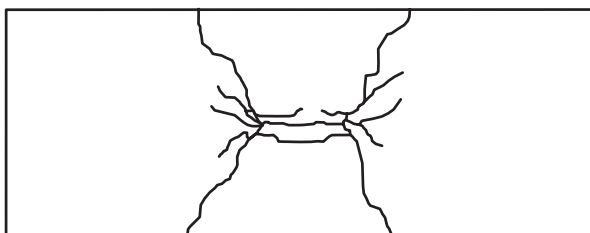


Fig. 10. Final crack pattern on underside of Collins' slab

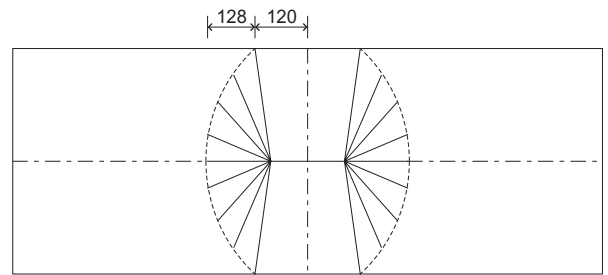


Fig. 11. Yield line pattern analysed by Collins

tension in the reinforcement away from the loading positions.

*Lower bound analysis.* The slab has been re-analysed using the methods described in this paper. To minimise the number of variables, one quarter of the slab was analysed, using the strip layout shown in Fig. 12. There are six different types of longitudinal strips (horizontal in the figure) and ten different type of transverse (vertical) strips, which means there are 60 different  $p_i$  values to be found. The loading patch was increased in size by adding one half of the slab thickness all round to allow for local load spreading. The moment capacities determined by Collins from material tests were used.

The program converged very slowly to a solution, and the highest lower bound found was 17.6 kN, some 33% lower than the lowest upper bound. Fig. 13 shows the moment distributions in the various strips. The top half of the figure shows the predicted bending moments in the six relatively weak longitudinal strips. The moments vary along the length but always remain within the hogging and sagging moment capacities, which are shown as the top and bottom of the boxes containing the bending moments. The lower half shows the variation in the ten transverse strips, which were much stronger in sagging bending than in hogging bending. The dominance of the sagging bending in the transverse direction under the load is clear, as is the absence of moment in the right hand half of the slab. In the area in between, however, where the fan mechanism developed, and as predicted by the yield line method, the situation

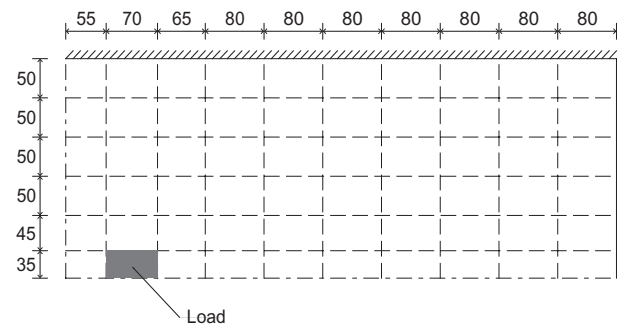


Fig. 12. Strip layout used to analyse Collins' slab (dimensions in mm). One quarter only of slab shown

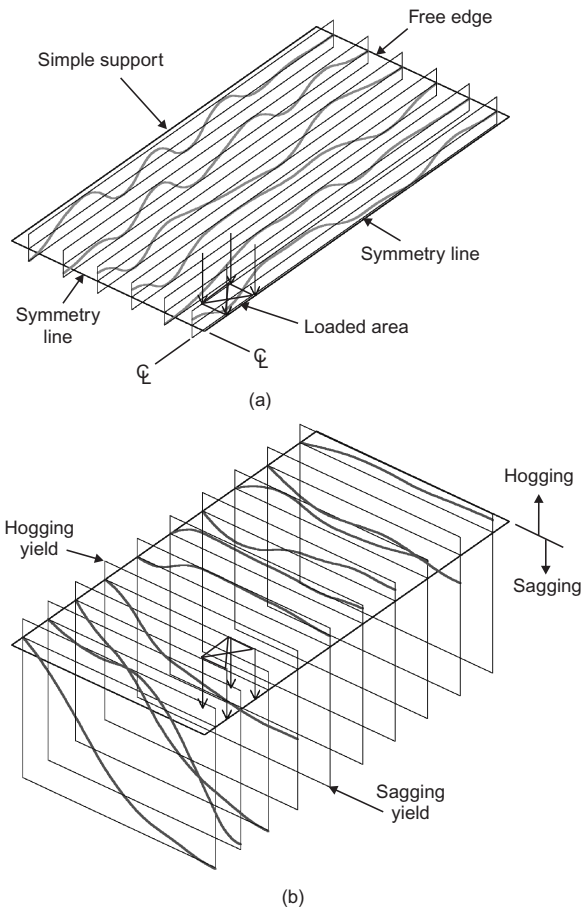


Fig. 13. Moment distributions in strip analysis of Collins' slab: (a) strips parallel to the support; (b) strips between supports. Only one quarter of the slab is shown for clarity

is far from simple, and no clear pattern can be discerned.

It is clear that the method, as presently constituted, is not good at determining when yielding takes place at an angle to the line of action of the strip. To see why that might occur, a case is needed for which good upper and lower bounds are known.

**Example 3. Fully fixed square slab**

One of the few non-trivial cases for which identical upper and lower bounds have been established is the clamped square slab (Fig. 14), which was analysed by Fox.<sup>10</sup> Both the distribution of moments for his lower bound and his upper bound collapse mechanism are necessarily complex, involving in the one case parabolic and hyperbolic moment distributions in the corners and in the other complex corner fans. The details are of no concern here, but his result is important. He showed that the true collapse load of the slab  $Q$  was given by  $QL^2/m_p = 42.85$ , where  $L$  is the span and  $m_p$  is the moment capacity per unit width in both sagging and hogging bending.

*Lower bound analysis results.* Figure 15 shows the layout used for the lower bound analysis, which

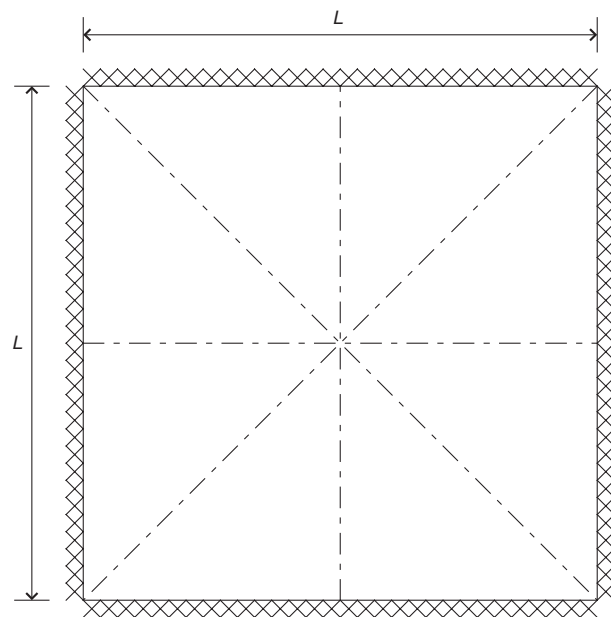


Fig. 14. Fully fixed square slab under uniformly distributed load, showing eight-fold symmetry

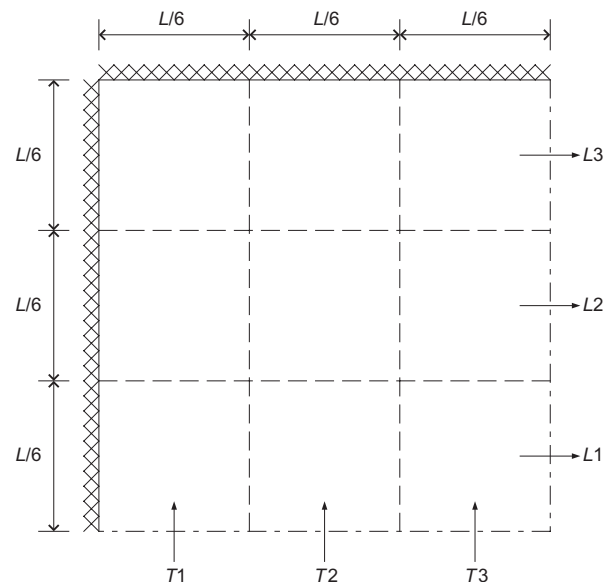


Fig. 15. Layout of strips used for lower bound analysis of example 3, showing strip divisions

was performed on a slab nominally 10 m square. Two lines of symmetry are enforced, and the resulting  $5\text{ m} \times 5\text{ m}$  slab divided into three longitudinal strips (L1, L2 and L3) and 3 transverse strips (T1, T2 and T3), giving nine values of  $p_i$  to be found. The program does not have the ability to enforce the diagonal symmetry, which could reduced the number of variables, although it was expected that this would emerge naturally from the answer.

The lower bound analysis predicts a maximum load of  $QL^2/m_p=32$ , but there are several different arrangements of  $\lambda_i$  that generate the same maximum. In each

case, all the strips are at yield in hogging at the supports and in sagging at midspan, although the bending moment distributions differ between strips as well as between the different  $\lambda_i$  distributions. This reflects the fact that there is no advantage in altering the moment distribution away from the yielding region; a similar phenomenon was observed in the previous example in the unloaded half of the slab.

The analysis has found the solution corresponding to a uniformly distributed load  $w$  applied to a fixed-ended beam with moment capacity  $m_p$ , which would give a collapse load of  $w = 16m_p/L^2$ . In the present case, half the load goes in each direction giving  $w = 32m_p/L^2$ .

It is possible that the routine has found a local maximum for  $Q$ , and that a higher global maximum exists but this cannot be checked without an exhaustive search, which would be prohibitively costly in computer time. Doubling (or even quadrupling) the number of strips in each direction does not alter the solution that is found.

Consideration of the failure patterns shows why this might be the case. Fig. 16 shows the 'yield line pattern' that would be suggested by the lower bound that is predicted here. Because the lower bound does not correspond to the true collapse load this pattern does not satisfy the compatibility conditions. Fig. 17 shows the classic yield line pattern for a clamped slab that does satisfy compatibility. It consists of diagonal sagging lines with corner fans. Even without the fans, this gives an upper bound of  $QL^2/m_p=48$  which is much closer to the true value than the lower bound produced here. It is immediately obvious that the two patterns differ widely. It is also obvious that a strip analysis, with strips running horizontally and vertically, will not have strips perpendicular to most of the yield lines, so cannot be

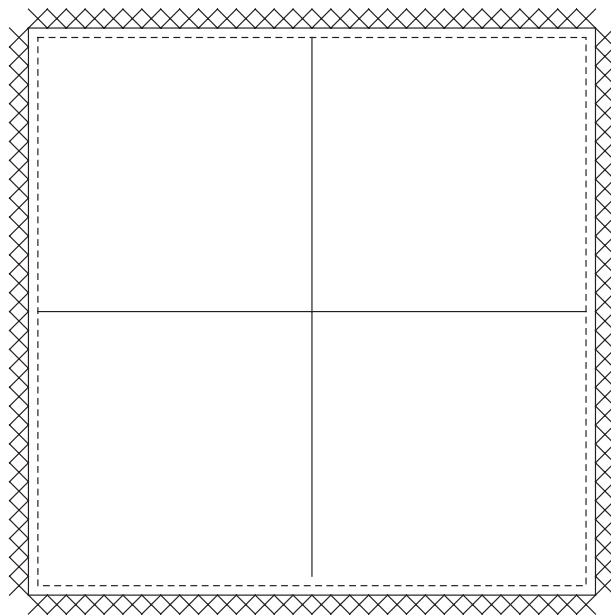


Fig. 16. Incompatible 'yield line pattern' predicted by lower bound analysis

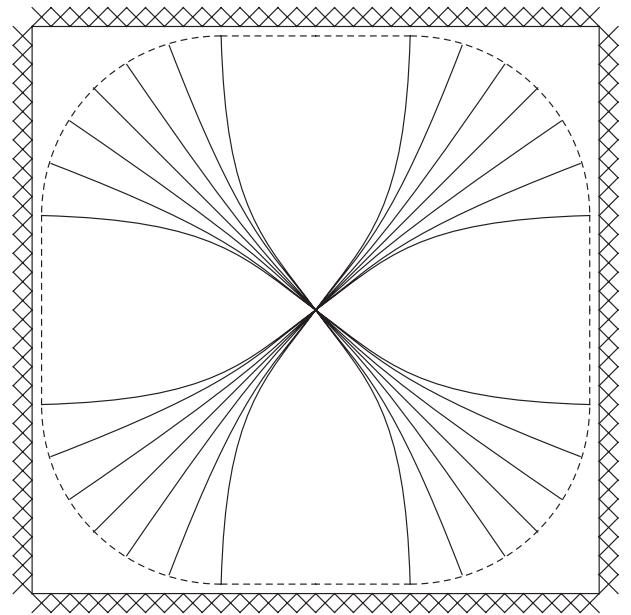


Fig. 17. Simplified corner fan yield line pattern

expected to have a stress field that is close to that which follows from the yield line pattern. It is thus unsurprising that the lower bound obtained by the strip method differs from the true solution, for the same reason that example 2 does not work well for the point loads.

In an attempt to overcome this problem, the slab was also analysed using strips parallel to the diagonals, as shown in Fig. 18. If load is shared equally between the two sets of strips, then the longest diagonal will govern and since it is  $\sqrt{2}$  longer than the side, the lower bound load will be halved to  $QL^2/m_p = 16$ . This can be improved if load is shared between the strips in a way that

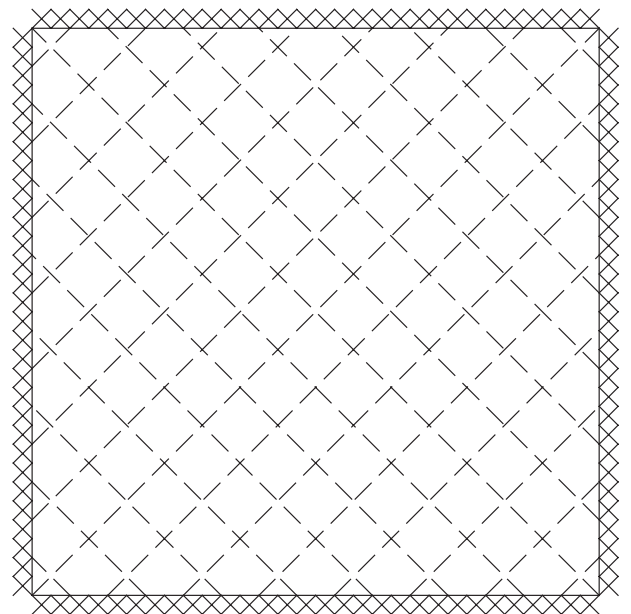


Fig. 18. Diagonal strips layout used for example 3

is linearly (although not proportionally) related to the relative stiffnesses of the two strips that cross at any point. Load can then be shed from long strips to short strips in the corners. The highest lower bound that has been found this way is  $QL^2/m_p=25.13$ . This is well below the collapse load predicted by having strips parallel to the sides.

Analogous effects have been noted before, but usually in connection with point loads, such as those imparted to flat slabs by supporting columns. Hillerborg<sup>11</sup> himself recognised the problem and introduced the idea of a rectangular corner-supported element which distributed the concentrated forces from the column to conventional strips elsewhere.

Rozvany<sup>12</sup> and Morley<sup>13</sup> introduced discontinuities in the moment field in two orthogonal directions, which allow the loads to be carried by diagonal shear forces towards the concentrated load. This overcomes the problem that axisymmetric moment patterns around a point load necessarily involve torsion, which is not allowed in Hillerborg strips. Rozvany also showed that the optimal design of slabs with corners required the use of diagonal strips spanning across the corners.

All of this work, and similar studies that followed, were concerned with the design problem, and have not been widely used in practice. Satisfactory designs can be produced without worrying about optimality conditions, and finite element methods, combined with the use of the Wood–Armer<sup>14</sup> equations, lead to structures that can safely carry the desired loads. But that is not the problem that is being addressed here where a good lower bound analysis technique is required. The fundamental problem is that the strip method is poor at distributing loads in directions that run at an angle to both sets of strips.

#### Analysis with four sets of strips

One way of introducing  $M_{xy}$  moments is to add strips at  $\pm 45^\circ$  to the original strips. The applied load can still be applied to one set of strips, as has been done in the previous analysis, but instead of one set of self-equilibrating inter-strip forces ( $p_i$  above) it will now be necessary to have three.

The question of the moment capacity has to be addressed. In the Hillerborg strip analysis it is assumed that there are two layers of steel, each of which contributes to the moment capacity in one set of strips; interactions between the strips can be conveniently ignored. With four sets of strips that will no longer be the case. For any given combination of the expanded set of inter-strip forces  $p_i$  it will be necessary to determine the corresponding moment triad ( $M_x, M_y, M_{xy}$ ) at any point of interest. This can then be compared with a suitable yield function so that the safe load multiplier can be determined.

To determine the ( $M_x, M_y, M_{xy}$ ) values at one point the values from four strips have to be combined, as shown in Fig. 19. Strips  $a-a$  and  $b-b$  are parallel to

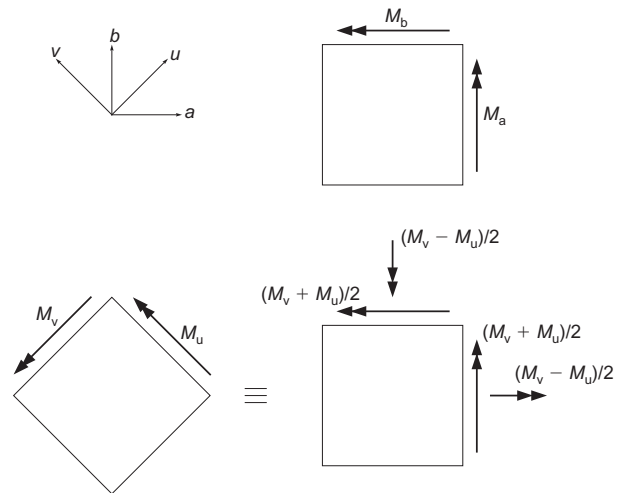


Fig. 19. Combining moments from four strips.

the  $x$ - and  $y$ -axes respectively, while  $u-u$  and  $v-v$  are at  $45^\circ$ . The lower part of the figure shows how the moments in the  $45^\circ$  elements are rotated to the  $0-90^\circ$  direction using Mohr's circle. To these must be added the moments from  $a-a$  and  $b-b$  to give the total moment field, which must be compared with the moment capacity described above. The resulting equations are

$$\begin{aligned} M_x &= M_a + \frac{(M_v + M_u)}{2} \\ M_{xy} &= \frac{(M_v - M_u)}{2} \\ M_y &= M_b + \frac{(M_v + M_u)}{2} \end{aligned} \quad (15)$$

The method can be applied to any suitable yield function. Denton and Burgoyne<sup>15</sup> presented a method of assessing the reserve moment capacity of a slab subjected to a given set of moments ( $M_x, M_y, M_{xy}$ ). That method differs from the Wood–Armer equations normally built into computer programs, which are intended for design of slabs and which include an optimality condition that is not required when performing an analysis. Other appropriate yield functions could be used. For example, May *et al.*<sup>16</sup> showed that, in certain circumstances, especially when  $M_{xy}$  moments were high, the Johanson yield criterion is unconservative. Because the method presented here checks the yield state at all points, it is possible to check whether May's yield condition should be substituted for the normal condition at any particular point. Deterioration, and thus reduced capacity, could also easily be checked provided that the program could be told how the reduced capacity would be distributed. It would also be possible to use an Ilyushin<sup>17</sup> or von Mises yield surface for analysing steel structures.

It should be noted that this analysis with four sets of strips only satisfies the moment capacity conditions at discrete points, which need to be predefined. When the

moment capacities of two strips are independent, as they are when only two orthogonal strips are used, the capacity can be checked at any point, but when four strips are used, various complications arise. The moment capacity has to be checked at locations where the moments in all four strips are known. The diagonal strips are not perpendicular to the supports, so the length of each strip varies. The refined method thus has to be applied to a regular square grid so that moments in each strip are calculated at the same point. It also means that a more accurate solution will be obtained by increasing the number of strips, at the expense of significantly increased computation time.

A revised version of the program has been written for the particular case of a square clamped plate under uniformly distributed load, and uses the Denton and Burgoyne approach, so the results should be directly comparable with Fox's exact solution and normal yield-line analyses. The program exploits the various symmetries in the slab so that only one quarter has to be analysed, but even so there are far more variables than when only two orthogonal strips are used, and each calculation is more complicated. Nevertheless, by dividing one quarter of a fixed plate into a  $6 \times 6$  grid, the highest lower bound found is  $QL^2/m_p = 41.19$ , which is much closer to Fox's value than that obtained with only two sets of strips. It is possible that this is not the highest lower bound that could be achieved with this layout of strips, but it does represent a valid lower bound on the collapse load of the slab.

Figure 20 shows the nodal locations where the slab is yielding at the highest lower bound found. Although directions of yielding are not shown, the pattern is remarkably similar to the exact form found by Fox.

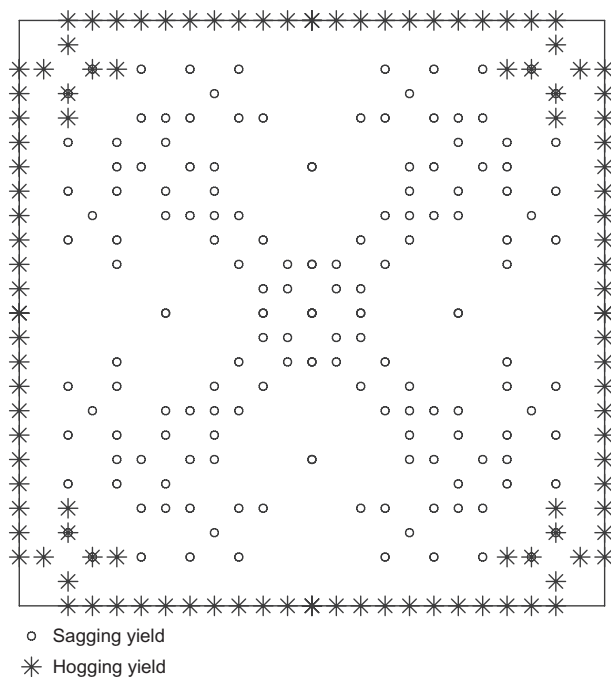


Fig. 20. Yielding locations in highest lower bound

### Other analyses of square slab

There have been many upper bound analyses of the square slab problem, several of which were summarised by Fox.<sup>10</sup> Wood's analysis<sup>18</sup> gave  $QL^2/m_p$  as 43.852; Mansfield<sup>19</sup> gave 42.895 and an improved version by Morley<sup>20</sup> gave 42.880, and although these patterns are simpler than that of Fox, they are too complicated for routine use. Analysis using an automated yield line program (COBRAS)<sup>5</sup> gives an upper bound of  $QL^2/m_p = 43.99$ , using the pattern shown in Fig. 21.

### Finite element analysis

An analysis of a square slab has also been carried out using a non-linear finite element program (Abaqus). This requires specific dimensions and material properties, and will also model membrane effects, so the results will not be exactly comparable to the other results quoted. The slab was modelled as a homogeneous material with an elastic modulus and moment capacity equivalent to a concrete slab with a single layer of reinforcement at mid-depth ( $E = 28$  GPa,  $m_p = 20$  kNm). The analysis of the slab using a fully non-linear procedure gave an ultimate collapse load of  $QL^2/m_p = 47.63$ , at which point both concrete crushing and steel yielding are taking place. This load is higher than the loads given by the upper bound solution, but is enhanced by the membrane action which both upper and lower bound methods ignore. If analysed using linear finite elements, as would normally be undertaken for assessment, the steel starts to yield at  $QL^2/m_p = 6.84$ , which shows how uninformative such programs can be. The load-deflection curve for the finite ele-

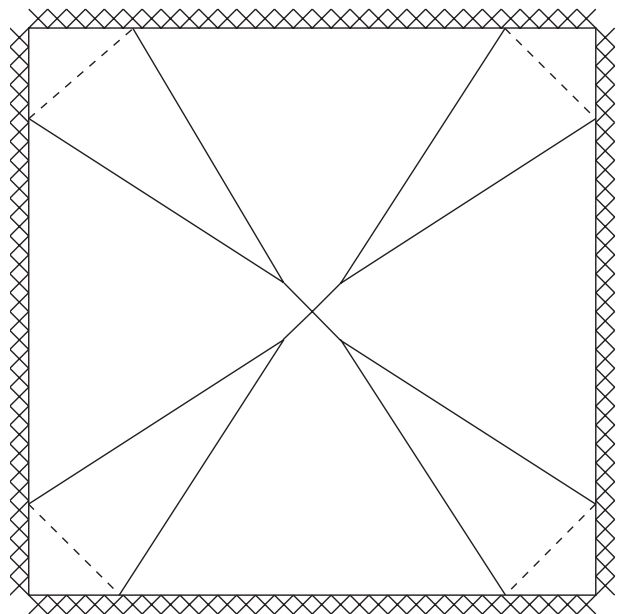


Fig. 21. Predicted yield line pattern for example 3 from COBRAS<sup>5</sup>

ment analysis is shown in Fig. 22, with the other bounds shown for comparison.

## Discussion

The results of all the different analyses and theories are shown in Table 1. As expected the upper and lower bounds bracket the exact solution. The COBRAS result is 3% high, and the lower bound method is 4% low. In real problems the exact solution is not known, so this method offers the real possibility of giving the checker some bounds on the degree of uncertainty about the slab's capacity.

The optimisation method used for this analysis is the same as that used when there are only two sets of strips, but the method converges very slowly, and it is by no means clear that the true optimum has been

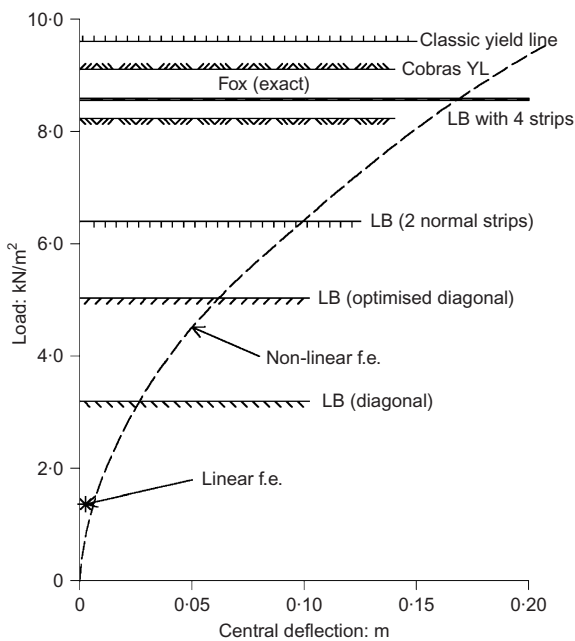


Fig. 22. Comparison of predictions for square slab under uniformly distributed load

Table 1. Values for  $QL^2/m_p$  using various analysis methods

Method	$QL^2/m_p$	Factor
Linear elastic finite element	6.84	0.160
Lower bound with simple diagonal strips	16	0.373
Lower bound with optimised diagonal strips	25.13	0.586
Lower bound with two strips parallel to sides	32	0.747
Lower bound with four strips	41.19	0.961
Fox's exact solution <sup>10</sup>	42.85	1
Best yield line: Mansfield <sup>19</sup> and Morley <sup>20</sup>	42.88	1.001
COBRAS yield line	43.99	1.026
Fully plastic finite element	47.63	1.112
Classic yield line analysis	48	1.120

reached. Hill-climbing techniques are greedy, in the sense that they walk as fast as possible up the nearest hill, and are likely to become stuck on a local maximum, or at a point from which they cannot escape. For more complex problems it would probably better be better to use an alternative technique, such as simulated annealing,<sup>7</sup> which has been used to solve the notorious 'travelling salesman' problem. This technique starts by allowing quite large random jumps in the various parameters (here the  $p_i$  values), and then slowly reducing the jump size as the solution is approached.

It is clear from the present work that the lower bound approach, although 'safe', is much harder to apply, because the structure is deemed to be at its capacity when yield is reached anywhere in the structure. Upper bound methods are not concerned with local failure; they only condemn the structure when a global failure mechanism can happen. This explains why, as observed in Fig. 22, all of the simple lower bounds significantly underestimate the load capacity, whereas even the worst upper bound is quite close to the true plastic collapse load. It also shows, however, the significant advantages that could be offered for the assessment of existing structures if the techniques described here could be generalised. Far fewer structures would be condemned, so much less unnecessary repair would be carried out, than when simple elastic analyses were performed.

## Conclusions

The following conclusions can be drawn from this study.

- It is possible to construct an automated procedure to analyse slabs using the Hillerborg strip method, which is normally used only for design.
- It is necessary to include self-equilibrating inter-strip forces to allow load to be transferred into strips that are otherwise unloaded.
- The load distribution within the slab can be expressed in terms of an equilibrium state and a set of states of self-stress. By varying the amount of each state of self-stress that is added, all valid combinations forces and moments that satisfy equilibrium can be described.
- A valid lower bound can be found from each of these equilibrium states.
- An automated procedure can be used to find the highest lower bound, but this must include a procedure to prevent the solution stopping at a non-optimal position.
- The method can be used to recover the assumptions made in the original design, even if those calculations are no longer available, which allows the method to be used for assessment of existing structures.
- Comparison with published values shows that low-

- er bounds can be calculated, but they may be well below the true collapse load of the structure. This is because the  $M_{xy}$  moments are being ignored.
- (h) By adding two additional sets of strips at  $\pm 45^\circ$  a higher lower bound can be obtained, which is much closer to the true collapse load.
  - (i) More care is needed when combining together the applied moments in four sets of strips since the moment capacities are no longer independent.
  - (j) The method is not restricted to one yield function.
  - (k) Lower bound methods are governed by local effects, whereas upper bound methods are governed by global effects.

## References

1. BURGUYNE C. J. Are structures being repaired unnecessarily? *The Structural Engineer*, 2004, **82**, No. 1, 22–26.
2. HILLERBORG A. Jämviksteori för armerade betongplattor (Equilibrium theory for concrete slabs). *Betong*, 1956, **41**, No. 4, 171–182.
3. HILLERBORG A. *Strip Method of Design*. Spon Press, London, 1976.
4. CALLADINE C. R. *Plasticity for Engineers, Theory and Applications*. Horwood, Chichester, 2000.
5. MIDDLETON C. R. Generalised collapse analysis of concrete bridges. *Magazine of Concrete Research*, 2008, doi: 10.1680/mac.2008.00091.
6. O'DWYER D. W. and O'BRIEN E. J. Design and analysis of concrete slabs using a modified strip method. *Structural Engineer*, 1998, **76**, No. 17, 329–333.
7. PRESS W. H., TEUKOLSKY S. A., VETTERLING W. T. and FLANNERY B. P. *Numerical Recipes in C++, The Art of Scientific Computing*, 2<sup>nd</sup> edn. Cambridge University Press, Cambridge, 2002.
8. REYNOLDS C. E. and STEEDMAN J. C. *Reinforced Concrete Designers Handbook*, 9<sup>th</sup> edn. Viewpoint, Slough, 1981.
9. COLLINS E. *Strength Assessment of Concrete Bridge Slabs with Low Transverse Reinforcement*. MEng Thesis, University of Cambridge, 1997.
10. FOX E. N. Limit analysis for plates: the exact solution for a clamped square plate of isotropic homogeneous material obeying the square yield criterion and loaded by uniform pressure. *Philosophical Transactions of the Royal Society of London, Series A*, 1974, **277**, No. 1265, 121–155.
11. HILLERBORG A. The advanced strip method: a simple design tool. *Magazine of Concrete Research*, 1982, **34**, No. 121, 175–181.
12. ROZVANY G. I. N. *Optimal Design of Flexural Systems*. Pergamon, Oxford, 1976.
13. MORLEY C. T. Equilibrium design solutions for torsionless grillages or hillerborg slabs under concentrated loads. *Proceedings of Institution of Civil Engineers, Part 2*, 1986, **81**, No. 3, 447–460.
14. WOOD R. H. The reinforcement of slabs in accordance with a predetermined field of moments. *Concrete*, 1968, **2**, 69–76 and correspondence by ARMER G. S. T, *Concrete*, 1968, **2**, 319–320.
15. DENTON S. R. and BURGUYNE C. J. The assessment of reinforced concrete slabs and bridge decks. *The Structural Engineer*, 1996, **74**, No. 9, 147–152.
16. MAY I. M., MONTAGUE P., SAMAD A. A. A., LODI S. H. and FRASER A. S. The behaviour of reinforced concrete elements subject to bending and twisting moments. *Proceedings of Institution of Civil Engineers, Structures and Buildings*, 2001, **146**, No. 2, 161–171.
17. BURGUYNE C. J. and BRENNAN M. G. Exact Ilyushin yield surface. *International Journal of Solids and Structures*, 1993, **30**, No. 8, 1113–1131.
18. WOOD R. H. *Plastic and Elastic Design of Slabs and Plates*. Thames and Hudson, London, 1961.
19. MANSFIELD E. H. Studies in collapse analysis of rigid-plastic plates with square yield diagram. *Proceedings of Royal Society of London, Series A*, 1957, **241**, No. 1226, 311–338.
20. MORLEY C. T. *The Ultimate bending Strength of Reinforced Concrete Slabs*. PhD Dissertation, University of Cambridge, 1965.

**Discussion contributions on this paper are welcomed by the editor**